Electric forces on a confined advacancy island

Frédéric Leroy, Ali El-Barraj, Fabien Cheynis, Pierre Müller, Stefano Curiotto

published in PHYSICAL REVIEW B 102 (2020) 235412
DOI: 10.1103/PhysRevB.102.235412

Electric forces on a confined *ad*vacancy island

F. Leroy,[1,*] A. El Barraj,[1] F. Cheynis,[1] P. Muller,[1] and S. Curiotto[1]
[1] *Aix Marseille Univ, CNRS, CINAM, Marseille, France*
(Dated: November 17, 2020)

The passage of an electric current in a material can cause a biased mass transport at its surface. This migration phenomenon is intimately related to the microscopic details of atomic processes of diffusion and attachment/detachment at step edges. Using low energy electron microscopy we have examined *in operando* under an electric current the migration of Si(111)-1×1 *ad*vacancy islands confined on Si(111)-7×7 terraces. The islands move opposite to the current direction, with velocity increasing with the radius. The effective valence of Si *ad*atoms is 2.8±0.5 and the kinetic length of attachment-detachment is about 500 nm. The analysis of the islands shape reveals that the electric current biases significantly the kinetic rate of mass transfers at step edges modifying the overall island shape.

Advances in the fabrication of nanostructures widely depend on the degree of knowledge of atomic processes at surfaces. In that respect atomic steps, as the most abundant structures at surfaces, play a key role in mass transfers. They are involved in complex atomic mechanisms such as the attachment-detachment of atoms or the atomic diffusion at the periphery of nanostructures [1 and 2]. To study the mass transfer mechanisms, different experimental strategies have been carried out based on the spatio-temporal fluctuations of the position of isolated/interacting steps [3–5] or on the step displacement velocity when a driving force intervenes using the fluctuation-dissipation theorem [6–8]. In particular the application of an electric current is known to bias the diffusion of mobile *ad*atoms. This effect, called electromigration [9–15], can cause substantial changes in the surface morphology such as step bunching for vicinal surfaces [16–19] or shape instabilities of 2D islands [20–24]. However it has been recently recognized that an electric current may not only impact *ad*atom diffusion but also atomic steps themselves by modifying their local properties such as the *ad*atom equilibrium concentration close to the step and/or the kinetic coefficients of attachment-detachment at step edges [5, 25, and 26]. These effects arise since the force acting on atoms depends on their local environment that differs at step edge, kink site or on top of a terrace. These local modifications of step properties are, to date, largely unknown whereas they are suspected to be extremely strong [5 and 25]. Moreover a better understanding of the effects of the electric current on surface mass transport gives also indirect information about the electric resistance of surfaces [27]. Indeed the electric forces acting on atoms, kink sites and step edges are compensated by opposite forces acting on charge carriers caused by these surface structures. These forces change the surface electric resistivity and may play a major role in electrical conductors when down-scaling in size [28 and 29]. This calls for specific studies on the effect of an electric current on the step properties and mass transport phenomena at the nanoscale.

In this letter we analyze quantitatively the atomic mechanisms of mass transport and step properties on Si(111) under an electric bias by addressing precisely the boundary conditions to disentangle all the contributions. In that purpose we have met two essential conditions: (1) An *ad*vacancy island where atomic displacements occur at the interior of a confined 2D space closed by a step edge; and (2) a driving force induced by an electric current to move the island. By adjusting the area of the island and measuring its drift velocity induced by an electric current we determine the mechanisms of mass transfers. This study is based on an *in operando* observation under an electric current of the Si(111) surface with low energy electron microscopy (LEEM). The experimental set-up allows to study the spatio-temporal dynamics of mass transfers at atomic steps [30]. We show a transition from a kinetics of mass transfer limited by attachment-detachment of atoms at step edges for small islands to a kinetics limited by terrace diffusion for large islands. We deduce that the kinetic length for attachment/detachment is $d \sim 500$ nm and the effective valence Z* of the Si *ad*atoms at the surface is 2.8±0.5. Importantly our detailed analysis of the stationary shape of the electromigrating *ad*vacancy islands is consistent with a strong modification of the local properties of attachment/detachment at step edges induced by the electric current.

The experiments were performed in an ultra high vacuum (UHV) setup equipped with a low energy electron microscope (LEEM III, Elmitec GmbH) [30]. Si(111) substrates (n or p-doped, ρ=1 Ωcm) were cut into pieces of 15×3×0.5 mm^3, cleaned with acetone and ethanol before introduction in UHV. An electric current is applied through the sample *via* two Mo electrodes clamped to its extremities. The samples were degassed in UHV for several hours at about 1100 K and then flashed above 1500 K for a few seconds by direct current heating. *Ad*vacancy islands are created by Si sublimation in the middle of large terraces [31]. The surface evolution under electromigration is studied by LEEM in bright field mode, with an electron beam energy of 3 eV. To change the *ad*vacancy islands size, Si was deposited *in situ* by a homemade direct current evaporator made of a piece of Si wafer clamped between Mo electrodes.

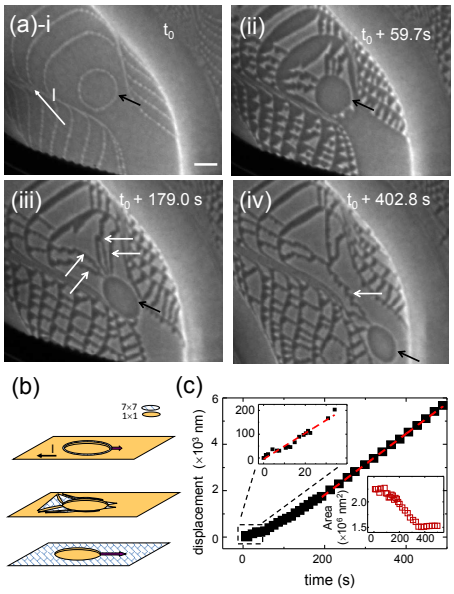

FIG. 1. (a) Sequence of LEEM images during the 1×1 → 7×7 phase transition and under electric heating (see complete movie S1 in the supplementary materials). (i) Nucleation of 7×7 surface reconstruction at the step edges on the upper terraces. (ii) Spreading of the 7×7 onto the terraces except in the *ad*vacancy island (black arrow) where the 7×7 nucleation is hindered. (iii) Formation of 1×1 out-of-phase boundaries at the 7×7 domain intersections (white arrows). (iv) Migration of the *ad*vacancy island in the $\langle\overline{1}12\rangle$ direction, opposite to the electric current. Out-of-phase boundaries merging at the rear side of the island. Electron energy E=3 eV. Scale bar 1μm. (b) Scheme of the surface evolution under slow cooling. (c) Time evolution of the displacement of the *ad*vacancy island (black square). The steady velocity is 13.1±0.1 nm.s^{-1} (velocity in (a)-i is 5.4±0.3 nm.s^{-1}, see top inset) and the area is 1.5±0.1 10^6 nm^2 (see bottom inset).

LEEM images in Fig. 1(a) show the time evolution of the Si(111) surface while crossing the 1×1 → 7×7 phase transition temperature (1133 K). The low temperature 7×7 surface reconstruction nucleates at the step edges on the upper terraces [32] and appears as bright lines (Fig. 1(a)-i). Upon slow cooling, by decreasing the electric current, the 7×7 phase extends onto the terraces (Fig. 1(a)-ii). Since the crystallographic arrangement of the different 7×7 domains does not necessarily coincide, 1×1 out-of-phase boundaries persist at their intersections. Moreover the nucleation of the 7×7 phase is hindered at the lower step edges and on terraces [7], therefore the *ad*vacancy island in the middle of Fig. 1(a)-iii stays in a metastable supercooled 1×1 state [33]. This effect was originally described as a hysteresis of the 1×1⟷ 7×7 phase transition temperature [34]. Interestingly this *ad*vacancy island migrates in the direction opposite to the electric current (Fig. 1(a)-iii-iv). During the displacement, the out-of-phase boundaries attached at the rear of the island merge from time to time and/or spontaneously detach. The velocity of the *ad*vacancy island increases up to 13.1± 0.1 nm.s^{-1} and reaches a stationary value when the 7×7 phase significantly covers the surrounding surface. Simultaneously, after an initial size reduction due to mass transfers with the exterior, the island size reaches also a steady state. Mass transfers have two contributions: The Gibbs-Thompson effect favors the capture of *ad*atoms as the *ad*vacancy island curvature is locally the largest one (in absolute). The phase transition expels the excess atoms of the 1×1 that diffuse to the step edge [35]. The fact that the island area stabilizes indicates that mass transfers from the exterior are nearly entirely suppressed when the 7×7 covers most of the surface. This diffusion barrier effect [36] is due to the large surface diffusivity of Si *ad*atoms on the 1×1 with respect to the 7×7 (ratio∼ 20, [7]). During its displacement the *ad*vacancy island can reach a step edge or a defect that may induce the nucleation of the 7×7 inside the island. To prevent this process from occurring the electric current direction is regularly reversed to change the drift direction by electromigration while keeping a constant temperature (±1 K). The islands move back and forth over a distance larger than 10 μm on extended terraces without meeting any surface defect or step (Fig. 2(b)). Concomitantly this process allows for the disappearance of all 1×1 out-of-phase boundaries attached to the islands by merging and detachment from the rear side and by removal at the front side. Let us note that a few out-of-phase boundaries have barely no effect on the measured velocity but their removal is important to determine the stationary shape of the *ad*vacancy island without ambiguity.

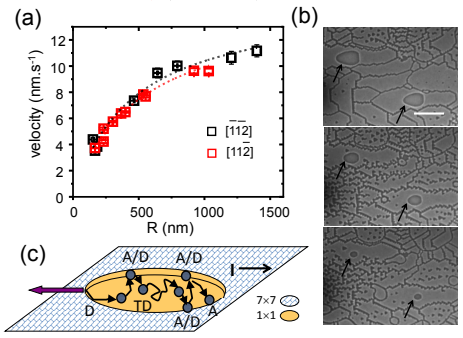

FIG. 2. (a) *Ad*vacancy island velocity versus radius. The islands electromigrate in the $\langle\overline{1}12\rangle$ (black square) and $\langle11\overline{2}\rangle$ (red square) directions. Fit of the velocity (dotted lines). (b) LEEM images of islands of different sizes electromigrating in the $\langle11\overline{2}\rangle$ direction (scale bar 5 μm, see complete movie S2 in the supplementary materials). (c) Scheme of mass transfer process: detachment of atoms (D), biased terrace diffusion (TD) and attachment (A).

To address the mass transport mechanisms that are occurring inside the *ad*vacancy islands under electromigration we have studied the size-dependence of the island velocity in the stationary regime. Figure 2(a) shows that the velocity increases with the island effective radius R ($R = \sqrt{A}/\pi$ where A is the island area). Pierre-Louis *et*

al. [20] have analyzed the island velocity in the framework of the linear response theory with weak electromigration. Considering a kinetics of mass transport by attachment (A), detachment (D) and terrace diffusion (TD) inside the 1×1 *ad*vacancy island (see Fig. 2(c)), and neglecting the *ad*atom flux from the upper terrace (7 × 7), the island drift velocity resulting from these processes is [20]:

$$V_{isl} = c_{eq} v_{1\times1} \frac{R}{R+d} \quad (1)$$

where c_{eq} is the equilibrium surface concentration of mobile *ad*atoms, $v_{1\times1}$ is the *ad*atoms velocity on the (1×1) terrace and $d = D_{1\times1}/k$ is the kinetic length of attachment/detachment and is defined as the ratio of the surface diffusion coefficient $D_{1\times1}$ to the rate k of *ad*atom attachment to the step from the terrace. Let us note that the mechanism of periphery diffusion of atoms along the step edge has been neglected since the velocity should decay as $1/R$ [20] and no evidence of this behavior is measured even for the smallest radius. The fit of the experimental plots give two key parameters $c_{eq}v_{1\times1}$ and d. The first term is deduced from the asymptotic velocity at large radius (15±1 nm.s^{-1}) and is only related to terrace diffusion of the electromigrating *ad*atoms. To estimate the *ad*atom velocity $v_{1\times1}$ we have to determine first c_{eq}. Since the step edge is hybrid, 1×1 reconstructed on the lower terrace and 7×7 on the upper one, the equilibrium concentration of *ad*atom close to the step edge is unknown. We have measured the *ad*atom concentration in the 1×1 *ad*vacancy island by decreasing the temperature to induce the $1\times1 \rightarrow 7\times7$ phase transition. The excess of *ad*atoms expelled by the phase transition condensates at step edges and shrinks the *ad*vacancy island area (see supplementary materials S3). The area fraction lost after the phase transition is 0.08 ± 0.02. Moreover considering that the 7×7 and the bulk-terminated 1×1 structure have a difference of atomic density of 0.04 [35], we can estimate that the density of mobile *ad*atoms of the 1×1 is 0.12 ± 0.02. As the steps on Si(111) are bilayers this corresponds to 0.24 ± 0.04 monolayer (ML) of *ad*atoms on the 1×1 surface of the *ad*vacancy island. This result is similar to 0.2 ML as estimated by [35] considering the 1×1 surface. This result is also consistent with the fact that the equilibrium concentration of *ad*atoms is a thermodynamic quantity. It is related to a difference of energy between two states: an atom attached at a step edge and on a terrace (*ad*atom). As the chemical environments of an atom attached to a 7×7 or 1×1 step edge are similar and very distinct from an *ad*atom on top of a 1×1 terrace, we expect that the step edge reconstruction only slightly modifies the equilibrium concentration. Using our experimental result of c_{eq} and correcting the velocity with *ad*vection [37] (sweeping effect on the *ad*atoms due to the step motion) we get finally the *ad*atom velocity $v_{1\times1} = 110 \pm 8$ nm.s^{-1} on the 1×1 surface reconstruction at the phase transition temperature. This velocity derives from the Einstein relation $v_{1\times1} = \frac{D_{1\times1}}{k_B T} F$ where k_B is the Boltzmann constant, T the temperature and $F = Z^* eE$ the electromigration force. Therefore the force and the effective charge Z^* of Si *ad*atoms can be obtained if the diffusion coefficient $D_{1\times1}$ is known. Hibino *et al.* have found $D_{1\times1}c_{eq} = 3.0\ 10^7$ s^{-1} [7 and 33] at the phase transition temperature. Pang *et al.* have obtained by different approaches $D_{1\times1}c_{eq} = 2.0 \pm 0.2\ 10^7$ s^{-1} [8] in a slightly higher temperature regime (1163 K). Considering an average value for $D_{1\times1}$ we can deduce $F = 1.4 \pm 0.3\ 10^{-6}$ eV.nm^{-1} and the only free parameter, *i.e.* the effective charge of Si *ad*atoms $Z^* = 2.8 \pm 0.5$ ($E = 490$ V.m^{-1}, atomic area: 0.064 nm^2). The deduced value of Z^* is larger by one order of magnitude with earlier reports [38 and 39] except for [40] ($Z^* > 1.3$). The model hypothesis of a weak electromigration is confirmed since the available thermal energy is much larger than the energy to electromigrate $\frac{Fa}{k_B T} \sim 10^{-5} \ll 1$ where $a = 0.384$ nm is the atomic lattice parameter [20]. The second term that is deduced from the fit is the kinetic length of attachment/detachment d. We obtain $d_{\langle 11\overline{2}\rangle} = 450 \pm 100$ nm and $d_{\langle \overline{1}\overline{1}2\rangle} = 500 \pm 30$ nm respectively for an island displacement in the $\langle 11\overline{2}\rangle$ and the $\langle \overline{1}\overline{1}2\rangle$ directions. It is interesting to note that, contrary to the equilibrium concentration that is close to the 1×1 surface, the kinetic length of attachment/detachment at the hybrid step edge is similar to the one measured at the step edges of the 7×7 reconstructed surface [41]. To explain this kinetic length we can note that, as for the 7×7 reconstructed surface, the advance of the hybrid step edge needs also to build 7×7 unit cells. This process is related to energy barriers and probably to the occurrence of concerted events that are necessary to achieve the complex mechanisms involved in the formation of a 7×7 unit cell [42 and 43]. From the evaluation of d we can estimate the rate of attachment/detachment at a step edge per atomic site $kc_{eq}a = c_{eq}D_{1\times1}a/d \sim 1.9 \times 10^4$ s^{-1}. It is also instructive to estimate the average macroscopic time for *ad*atoms to detach from the front side, cross the island and attach at the rear side. The traveling time across the terrace by diffusion is about $t_d \sim 2R/v_{1\times1}$ and for a typical island of 1 μm radius $t_d \sim 15$ s. As a comparative time scale, the delay time for an atom to make all attachment/detachment processes to cross the island is about $t_{AD} \sim 2d/v_{1\times1} \sim 6$ to 8 s. This indicates that many events of (re)-attachment-detachment occur during this traveling ($kc_{eq}a \times t_{AD} \sim 10^5$, see Fig.2(c)).

In addition to velocity, the *ad*vacancy island shape in the stationary regime is measured and depends both on the island size and electric current direction. In Fig. 3(a), the *ad*vacancy islands have a facetted front and an overall triangular shape when they migrate in the $\langle 11\overline{2}\rangle$ direction whereas they have a lozenge shape (elongated head and lateral facets) in the opposite direction. If they move in the $\langle \overline{1}10\rangle$ direction the shape is no more symmetric (Fig. 3(d)). In all cases the shape is elongated in the migration direction. This elongation increases with the island size and tends to be circular for small sizes (the

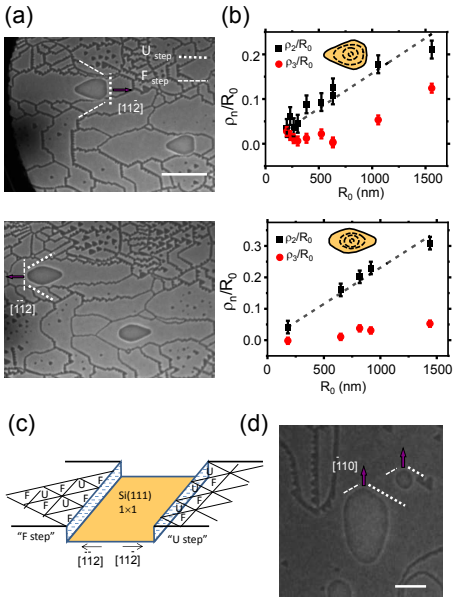

FIG. 3. (a) LEEM images of *ad*vacancy islands electromigrating in the $\langle 11\bar{2}\rangle$ (top) and the $\langle \bar{1}12\rangle$ (bottom) directions (scale bar 5 μm). The shape is respectively a triangle and a lozenge. Unfaulted steps (U_{step}) are shown as dotted lines and faulted steps (F_{step}) as dashed lines [44]. (b) Fourier coefficients of the island shape as function of island radius for both direction. (c) Scheme of the U and F step edge structure. (d) LEEM image of two *ad*vacancy islands electromigrating in the $\langle 1\bar{1}0\rangle$ direction. The shape is asymmetric (scale bar 1 μm, see complete movie S4 in the supplementary materials).

typical crossover is about the attachment-detachment kinetic length d). To describe the island shape, we use the polar coordinates $R(\theta) = R_0 + \rho(\theta)$ (R_0 is the mean radius), and we apply the Fourier series expansion of $\rho(\theta)$:

$$\rho(\theta) = \sum_{n\geq 2}^{\infty} \rho_n \cos(n\theta) + \nu_n \sin(n\theta) \qquad (2)$$

where ρ_n and ν_n are the Fourier coefficients ($\nu_n = 0$ for symmetric islands and ρ_1 and ν_1 are not considered because they correspond to a simple shape translation). In Fig. 3(b) are plotted the normalized Fourier coefficients ρ_n/R_0 as function of the island radius R_0 when the islands are migrating along the $\langle 11\bar{2}\rangle$ and $\langle \bar{1}12\rangle$ directions. The main term of elongation is the n=2 mode ρ_2/R_0 and in both cases it increases approximately linearly with the island radius. ρ_2/R_0 is larger when the island has a lozenge shape. The triangular shape of the islands migrating in the $\langle 11\bar{2}\rangle$ direction is given by a strong n=3 mode ρ_3/R_0 that is increasing non-linearly with the island radius.

Our first insight into the island shape and symmetry is based on crystallographic considerations. The step edge properties of the 7×7 have a threefold symmetry [45 and 46]. However due to symmetry breaking by electromigration, maximum a mirror symmetry can be expected. As observed experimentally if the electric current is along the symmetry axis $\langle 11\bar{2}\rangle$ the shape has a mirror line whereas it is not the case when the electric current is along the non-symmetric $\langle \bar{1}10\rangle$ direction (Fig. 3(d)). As the shape is far from equilibrium the kinetic of mass transfers such as the one involved in the attachment/detachment of atoms at step edges is expected to play a major role.

In the framework of a continuous step model with isotropic surface properties, the shape of *ad*vacancy islands driven by an electromigration force on *ad*atoms and considering mass transfers by terrace diffusion and attachment/detachment at step edges has been calculated [20, 24, and 37]. The elongation of the *ad*vacancy islands is perpendicular to the migration direction. This shape can be qualitatively interpreted as resulting from a mass flux towards the migration axis. Indeed in presence of a slow kinetics of attachment, the *ad*atoms make several trials before attaching to the step and have a residual drift towards the migration axis. In a steady state the local curvature of the island is modified to compensate this mass flux by a capillary effect. Quantitatively the change of shape involves the $n = 2$ mode as ρ_2/R_0 ratio (elongation) and reads ([20] for $d \ll R_0$):

$$\frac{\rho_2}{R_0} = -\frac{1}{12\Gamma}\frac{R_0^2}{\xi^2} d < 0 \qquad (3)$$

where $\Gamma = \frac{a^2\tilde{\beta}}{k_B T}$ is the capillary length (Gibbs-Thomson effect), $\tilde{\beta}$ is the step edge stiffness and ξ is a characteristic length associated with the electromigration force ($\xi = \frac{k_B T}{F} = 70$ μm). This result is opposite to the experimental shape since the elongation of the *ad*vacancy islands is along the migration direction ($\frac{\rho_2}{R_0} > 0$). As this result is observed whatever the direction of the electric current we infer that even if the modeling could include the anisotropy of the surface properties, it alone could not explain that the shape is always elongated along the migration axis. Therefore we propose that the electric current modifies not only the *ad*atom displacement but also the atomic step properties. As a minimum model, the electric current breaks the threefold symmetry of the kinetic rate of attachment-detachment at the step edges [47]. To study this effect we expand the kinetic length d as a Fourier series $d = \overline{d} + \sum_n d_n cos(n\theta)$ where $\overline{d}$ is the mean kinetic length of attachment/detachment and d_n are the Fourier coefficients for a symmetric shape. The main Fourier term acting as an electrobias, *i.e.* changing the kinetics of attachment-detachment at the step edge, is expected to be d_1 since it breaks the symmetry between the island front where the current is step-down and the island rear where the current is step-up. Let us note that without electrobias only d_{3n} exists by symmetry. Expanding linearly the shape of the *ad*vacancy island with this electrobias effect we obtain:

$$\frac{\rho_2}{R_0} = -\frac{1}{12\Gamma}\left[\frac{R_0^2}{\xi^2}\left(\overline{d} + \frac{d_2}{2}\right) - 2\frac{R_0}{\xi}(d_1 + d_3)\right] \qquad (4)$$

The shape elongation $\frac{\rho_2}{R_0}$ shows a new contribution that increases linearly with the island radius R_0 as in the measurements, and is along the migration axis if $d_1 + d_3 > 0$. As $\frac{R_0}{\xi} \sim 0.014 \ll 1$ we can neglect the second order contribution in eq. (4). To estimate only the electrobias effect d_1 we use the change of the current direction in the experiment. Assuming that d_3 is not significantly affected by the electrobias effect, since it is a three order term in the series expansion and do not coincide with the symmetry of the electric current, the inversion of the current direction changes d_3 by $-d_3$ [48]. Therefore the kinetic length of electrobias d_1 is obtained by averaging both shape elongation $\frac{\rho_2}{R_0}$ in the $\langle 11\overline{2}\rangle$ and the $\langle \overline{11}2\rangle$ directions. We estimate that $d_1 \sim 83 \pm 12$ nm (Γ =1 nm [8]) and considering that this contribution is thermally activated, we extract the activation energy $E_1 = k_B T \ln\left(1 + \frac{d_1}{\frac{a}{2}}\right)$ =1.5 10^{-2} eV. This electrobias effect on the step edge is much larger than on *ad*atoms ($E = Fa/2$ ~2.6 10^{-7} eV). This result could be related to an intrinsic change of step properties induced by the current but it may also arise from a change of kink density at step edges. Indeed it has been shown [49] that an electric current in the $\langle 11\overline{2}\rangle$ direction along a step and ascending the kinks favors the formation of an atomically straight step edge. Therefore considering that the kinetics of mass transfers at step edges is mediated by kinks then the rate of attachment/detachment could be indeed strongly modified by the electric current. Such an electrobias effect on step edges or kink sites has been suspected to occur on semiconductor surfaces [50]. On metals a similar electrobias effect has also been found. However the studies on Ag metal [5 and 25] have addressed a different regime of mass transport dominated by atomic diffusion along the island periphery. The electrobias effect was studied considering a different methodology based on the analysis of step fluctuations and island velocity but not on the island shape whereas it is strongly sensitive to the local modifications of the step edge properties [20].

In conclusion we have shown on Si(111) surface that an *ad*vacancy island in the 1×1 high temperature phase and surrounded by the 7×7 low temperature phase can be stabilized. This regime allows keeping the 2D island in a confined state in terms of atomic exchanges. Then under the influence of an electric current, the island is moving. The analysis of the velocity and shape of the island as function of its radius show that (i) Si *ad*atoms migration on the terrace is biased and they have an effective valence Z^* of 2.8±0.5 (ii) the kinetic of attachment/detachment of atoms at the step edges is very slow and we evaluate the kinetic length as ~ 500 nm. (iii) An electrobias effect on the kinetics of attachment/detachment at step edges elongates the island shape in the direction of the electric current. We believe that a complete modeling including all the effects of anisotropy, non-linearities and high density of *ad*atoms would be necessary to describe precisely the island shape.

We are grateful to Olivier Pierre-Louis for instructive discussions and Plateform PLANETE (CNano PACA) for technical support. This work has been supported by the ANR grant HOLOLEEM (ANR-15-CE09-0012).

* leroy@cinam.univ-mrs.fr

[1] Hyeong-Chai Jeong and Ellen D Williams. *Surf. Sci. Rep.*, 34(6-8):171–294, 1999.

[2] Chaouqi Misbah, Olivier Pierre-Louis, and Yukio Saito. *Reviews of Modern Physics*, 82(1):981–1040, 2010.

[3] N. C. Bartelt, J. L. Goldberg, T. L. Einstein, Ellen D. Williams, J. C. Heyraud, and J. J. Métois. *Physical Review B*, 48(20):15453–15456, 1993.

[4] DB Dougherty, I Lyubinetsky, ED Williams, M Constantin, C Dasgupta, and S Das Sarma. *Physical Review Letters*, 89(13):136102, 2002.

[5] O. Bondarchuk, W. G. Cullen, M. Degawa, E. D. Williams, T. Bole, and P. J. Rous. *Physical Review Letters*, 99(20):206801, 2007.

[6] K. Thurmer, J.E. Reutt-Robey, E.D. Williams, M. Uwaha, A. Emundts, and H.P. Bonzel. *Physical Review Letters*, 87(18):186102, 2001.

[7] H. Hibino, C.-W. Hu, T. Ogino, and I. S. T. Tsong. *Physical Review B*, 63(24):245402, 2001.

[8] A. B. Pang, K. L. Man, M. S. Altman, T. J. Stasevich, F. Szalma, and T. L. Einstein. *Physical Review B*, 77(11):115424, 2008.

[9] H. B. Huntington and A. R. Grone. *J. Phys. Chem. Solids*, 20:76, 1961.

[10] I. A. Blech. *J. Appl. Phys.*, 47(4):1203–1208, 1976.

[11] A. H. Verbruggen. *IBM J. Res. Dev.*, 32(1):93–98, 1988.

[12] P. S. Ho and T. Kwok. *Rep. Prog. Phys.*, 52(3):301–348, 1989.

[13] H. Yasunaga and A. Natori. *Surf. Sci. Rep.*, 15(6-7):205–280, 1992.

[14] S. Curiotto, F. Cheynis, P. Müller and F. Leroy. *ACS Appl. Nano Mater.*, 3(2):1118–1122, 2020.

[15] S. Curiotto, P. Müller, A. El Barraj, F. Cheynis, O. Pierre-Louis and F. Leroy. *Appl. Surf. Sci.*, 469:463–470, 2019.

[16] A.V. Latyshev, A.L. Aseev, A.B. Krasilnikov, and S.I. Stenin. *Surface Science*, 213(1):157–169, 1989.

[17] Y Homma, RJ McClelland, and H Hibino. *Jpn. J. Appl. Phys.*, 29(12):L2254–L2256, 1990.

[18] F. Leroy, P. Müller, J. J. Metois, and O. Pierre-Louis. *Phus. Rev. B*, 76(4), 2007.

[19] F. Leroy, D. Karashanova, M. Dufay, J. M. Debierre, T. Frisch, J. J. Metois, and P. Müller. *Surf. Sci.*, 603(3):507–512, 2009.

[20] O. Pierre-Louis and T. L. Einstein. *Phys. Rev. B*, 62(20):13697–13706, 2000.

[21] Philipp Kuhn, Joachim Krug, Frank Hausser, and Axel Voigt. *Physical Review Letters*, 94(16):166105, 2005.

[22] A. Kumar, D. Dasgupta, C. Dimitrakopoulos, and D. Maroudas. *Appl. Phys. Lett.*, 108(19):193109, 2016.

[23] A. Kumar, D. Dasgupta, and D. Maroudas. *Physical Review Applied*, 8(1):014035, 2017.

[24] Stefano Curiotto, Frédéric Leroy, Pierre Müller, Fabien

Cheynis, Ali El-Barraj, Michail Michailov, and Bogdan Ranguelov. *J. Cryst. Growth*, 520:42–45, 2019.

[25] C. Tao, W. G. Cullen, and E. D. Williams. *Science*, 328(5979):736–740, 2010.

[26] Kirk H. Bevan, Hong Guo, Ellen D. Williams, and Zhenyu Zhang. *Physical Review B*, 81(23):235416, 2010.

[27] E. D. Williams, O. Bondarchuk, C. G. Tao, W. Yan, W. G. Cullen, P. J. Rous, T. Bole. *New Journal of Physics*, 9(10):387, 2007.

[28] Bruno V.â C. Martins, Manuel Smeu, Lucian Livadaru, Hong Guo, and Robert A. Wolkow. *Physical Review Letters*, 112(24):246802, 2014.

[29] Sven Just, Marcus Blab, Stefan Korte, Vasily Cherepanov, Helmut Soltner, and Bert VoigtlÃnder. *Physical Review Letters*, 115(6):066801, 2015.

[30] F. Cheynis, F. Leroy, A. Ranguis, B. Detailleur, P. Bindzi, C. Veit, W. Bon, and P. Müller. *Review of Scientific Instruments*, 85:043705, 2014.

[31] Yoshikazu Homma, Hiroki Hibino, Toshio Ogino, and Noriyuki Aizawa. *Physical Review B*, 55(16):R10237–R10240, 1997.

[32] N Osakabe, Y Tanishiro, K Yagi, and G Honjo. *Surface Science*, 109:359–366, 1981.

[33] H. Hibino, Y. Watanabe, C.-W. Hu, and I. S. T. Tsong. *Physical Review B*, 72(24):245424, 2005.

[34] C.-W. Hu, H. Hibino, T. Ogino, and I. S. T. Tsong. *Surface Science*, 487:191–200, 2001.

[35] Y.-N. Yang and E. D. Williams. *Physical Review Letters*, 72(12):1862–1865, 1994.

[36] H. Hibino, C.-W. Hu, T. Ogino, and I. S. T. Tsong. *Physical Review B*, 64(24):245401, 2001.

[37] Frank Haußer, Philipp Kuhn, Joachim Krug, and Axel Voigt. *Physical Review E*, 75(4):046210, 2007.

[38] Daniel Kandel and Efthimios Kaxiras. *Physical Review Letters*, 76(7):1114–1117, 1996.

[39] E.S. Fu, D.J. Liu, M.D. Johnson, J.D. Weeks, and E.D. Williams. *Surface Science*, 385:259–269, 1997.

[40] Andrés Saùl, Jean-Jacques Métois, and Alain Ranguis. *Physical Review B*, 65(7):075409, 2002.

[41] W. F. Chung and M. S. Altman. *Physical Review B*, 66(7):075338, 2002.

[42] Wataru Shimada, Tomoshige Sato, and Hiroshi Tochihara. *Physical Review B*, 94(3):035402, 2016.

[43] Ing-Shouh Hwang, Mon-Shu Ho, and Tien T Tsong. *Physical Review Letters*, 83(1):120, 1999.

[44] H. Tochihara, W. Shimada, M. Itoh, H. Tanaka, M. Udagawa, and I. Sumita. *Physical Review B*, 45(19):11332–11335, 1992.

[45] Noriko Akutsu and Yasuhiro Akutsu. *Journal of Physics: Condensed Matter*, 11(35):6635–6652, 1999.

[46] Noriko Akutsu. *Surface Science*, 630:109–115, December 2014.

[47] Nobuo Suga, Junya Kimpara, Nan-Jian Wu, Hitoshi Yasunaga, and Akiko Natori. *Japanese Journal of Applied Physics*, 39(Part 1, No. 7B):4412–4416, July 2000.

[48] Considering the general case where d_3 is also affected by the electric current we obtain by current reversal the quantity $d_1 + d_3^{el}$ in Eq.(4) where d_3^{el} is the specific contribution of the electric current on d_3.

[49] S. Yoshida, T. Sekiguchi, and K. M. Itoh. *Applied Physics Letters*, 87(3):031903, 2005.

[50] Mon-Shu Ho, Ing-Shouh Hwang, and Tien T. Tsong. *Physical Review Letters*, 84(25):5792–5795, 2000.